Arabian Journal of Chemistry (2020) **13**, 5406–5416

King Saud University

Arabian Journal of Chemistry

www.ksu.edu.sa
www.sciencedirect.com

ORIGINAL ARTICLE

Development of reproducible thiourea sensor with binary SnO_2/V_2O_5 nanomaterials by electrochemical method

M.M. Alam [a,*], M.T. Uddin [a], Abdullah M. Asiri [b,c], Mohammed M. Rahman [b,c,*], M.A. Islam [a]

[a] *Department of Chemical Engineering and Polymer Science, Shahjalal University of Science and Technology, Sylhet 3100, Bangladesh*
[b] *Chemistry Department, King Abdulaziz University, Faculty of Science, P.O. Box 80203, Jeddah 21589, Saudi Arabia*
[c] *Center of Excellence for Advanced Materials Research, King Abdulaziz University, P.O. Box 80203, Jeddah 21589, Saudi Arabia*

Received 11 February 2020; accepted 22 March 2020
Available online 4 April 2020

KEYWORDS

Thiourea sensor;
Binary mixed SnO_2/V_2O_5 nanomaterials;
Pathological diagnosis;
Wet-chemical method;
Healthcare safety

Abstract In this methodology, the thiourea (TU) sensor was made-up by means of glassy carbon electrode (GCE) layered by the wet-chemically prepared binary SnO_2/V_2O_5 nanomaterials (NMs). The existence of SnO_2 and V_2O_5 in prepared spherical NPs were categorized by X-ray photoelectron spectroscopy (XPS), Field Emission Scanning Electron Microscopy (FESEM), Energy-dispersive X-ray spectroscopy and X-ray Powder Diffraction (XRD). The TU sensor was displayed the linear responses in concentration range (LDR) of 0.1 nM ~ 0.01 mM. The calibration curve of TU sensor was made by plotting current verses concentration of TU, which was measured by electrochemical technique. The sensitivity and lower limit of detection (DL) for TU sensor were calculated from calibration curve, which are found as 17.0918 $\mu A \mu M^{-1} cm^{-2}$ and 95.40 ± 4.77 pM respectively. The analytical parameters of TU sensor such as reproducibility, response time and stability were measured and found efficient results. It also was validated in the detection of TU in presence of real biosamples. Thus, this unique and prospective method is introduced to develop the selective biosensor by electrochemical approach, which might be a pioneer sensor probe for its simple and reliable approach for the safety of healthcare and biomedical fields in a large scales.

* Corresponding authors at: Chemistry Department, King Abdulaziz University, Faculty of Science, P.O. Box 80203, Jeddah 21589, Saudi Arabia (M.M. Rahman).
E-mail addresses: alam-mahmud@hotmail.com (M.M. Alam), mmrahman@kau.edu.sa (M.M. Rahman).
Peer review under responsibility of King Saud University.

Production and hosting by Elsevier

https://doi.org/10.1016/j.arabjc.2020.03.019

1. Introduction

The thiourea is valuable organosulfur compound and has numerous application in science and technology. For electrodeposition of metals, rubber vulcanization, cleaning, agrochemicals, medicine, veterinary medicine and food industries, thiourea (TU) has been found to usage extensively (De Oliveira et al., 2004; Moragues et al., 2012; Lin et al., 2011). To inhabit browning of horticultural products, TU is an useful substance (Siddiq et al., 1994; Gilly et al., 2001). In agricultural sector, TU is an effective agrochemical used to protect early ripening of various fruits and breaking seeds and tubers dormancy (Sohan et al., 1991; Ezekiel et al., 2000; Gholap et al., 2000; Karam and Al-Salem, 2001; Khan and Ungar, 2001). Besides this, TU is used as fungicide in cold storages for preserving citrus fruits (WHO, 2000). According to Unite State Department of Health and Human Services, TU has been categorized as carcinogenic chemical (US Department of Health and Human Services, 1985). Therefore, it should be avoided to exposure or contamination of environment from thiourea. Due to exposure of thiourea, it is responsible for Hypothyroidism syndrome in human (Sokkar et al., 2000; Bhide et al., 2001). So, TU is well known as antithyroid drug and it has been used to manage hyperthyroidism in human since last decade (Cooper, 1984; Heidari et al., 2015). Considering the coincidence of TU, it is necessary to analysis food, portable water and environment for ensuring optimum level of TU. The existing methods for determination of TU are FTIR (Kargosha et al., 2001), titration with mercury (II) chloride (Kies, 1978) and HPLC (Rethmeier et al., 2001) are famous. A number of disadvantages are associated with these existing methods such as expensive and heavy instrumentation (HPLC, FT-IR), costly reagent needed (HPLC), time consuming (HPLC, titrations) and lower sensitivity (FTIR, titrations). Recently, the electrochemical technique is prevalent due to its attractive advantages such as inexpensive and simple instrumentation, short analysis time with high sensitivity and in-situ determination. As a result, a number researches have been reported using metal oxides as sensing element to determination of various environmental toxic chemical reliably (Rahman et al., 2018a; Alam et al., 2018a; Awual et al., 2019a; Hussain et al., 2016).

To determination of toxic chemicals in electrochemical approach, the electrochemical properties of sensing transition and semi-conductive metal oxides are main objectives. SnO_2 is well known n-type semi-conductor having wider band-gap energy (3.64 eV). With the attractive physical, chemical and electronic properties of SnO_2, it has been found to apply in various application such as catalysts (You et al., 2009), lithium batteries (Bose et al., 2002), gas sensor (Kennedy et al., 2003) and fuel cell (Guo, 2010). Besides this, SnO_2 has been reported as chemical sensor for determination of acetone (Rahman et al., 2017a), benzaldehyde (Subhan et al., 2018a), creatine (Rahman et al., 2017b) and hydrazine (Rahman et al., 2016a) in buffer phase applying electrochemical approach. The V_2O_5 is n-type semi-conducting metal oxide and it has appealed great attraction due to its outstanding properties including optical band gap (2.3 eV) energy, potential thermoelectric properties, good thermal and chemical stability (Wruck et al., 1989; Kosacki et al., 1992; Schneider et al., 2016). Thus, it is found to apply in various technological application such as lithium ion battery (Wang et al., 2006; Pyun and Bae, 1996), super-capacitors and energy storage gadgets (Portion et al., 1999; Le Van et al., 2006; Ramana et al., 2005) and gas sensors of hydrogen (Baik et al., 2009; Byon et al., 2012). It has been reported that the binary composite of nano-hetero-structured metal oxides are very effective in gas sensing applications (Zhang et al., 2019; Zhang et al., 2020; Rahman et al., 2015). The goal of this present study was to investigate the binary combination of n-type semiconductive SnO_2 and V_2O_5 as electrochemical sensor to detect toxic chemical in buffer phase.

To conduct this investigation, the NMs of SnO_2/V_2O_5 were produced by means of the wet-chemical (co-precipitation) technique in alkaline phase and the proposed sensor was made-up by coating of a GCE as thin uniform layer with slurry of SnO_2/V_2O_5 NMs. The suggested sensor was found to selective toward the thiourea. The details investigation for TU sensor was executed in-term of detection limit, sensitivity, reproducibility, linear dynamic range, long-term stability and response time and all the resulted analytical performances of TU sensor were exhibited satisfactory and reliability. Besides this, it was validated in detection of TU in real bio-samples. Considering the advances of TU sensor instead of tradition detection method of TU, this methodology will be unique and pioneer in the field of sensor development.

2. Experimental

2.1. Chemical reagents and methods

To prepare SnO_2/V_2O_5 NMs, the Tin (II) chloride ($SnCl_2{\cdot}2H_2O$) and Vanadyl sulfate ($VOSO_4{\cdot}5H_2O$) in analytical grade were procured from Sigma-Andrich Company. The concentrated ammonium, mono- & disodium phosphate and nafion (5% in ethanol) were also bought from the same Sigma-Andrich company. As a part of this study, thiourea (TU), 4-nitrophenylhydrazine (4-NPHyd), 3-methoxyphenylhydrazine hydrochloride (3-MPhydHCl), chloroform, 1,2-diaminobenzene (1,2-DAB), 1,4-dioxane, 3-chlorophenol (3-CP), acetylpyridine (APy) and 3-methoxyphenol (3-MP) were applied as analytes to execute this study. For the detail characterization of SnO_2/V_2O_5 NMs, XPS (Thermo Scientific), Powder X-ray Diffraction (XRD), FESEM (Field-emission Scanning Electron Microscope) attached with EDS facility were applied. The electrochemical behavior of synthesized nanomaterials were evaluated using Keithley Electrometer (USA).

2.2. Synthesized of SnO_2/V_2O_5 NMs applying wet-chemical process

The wet-chemical (co-precipitation) is the simplest and oldest method to preparation of metal oxide or mixture of metal oxides in nanoscale. This method was implemented to prepare SnO_2/V_2O_5 NMs. Following this technique, 0.1 M $VOSO_4{\cdot}5H_2O$, 0.1 M $SnCl_2{\cdot}2H_2O$ and 0.1 M NH_4OH were formed in demineralized water into three individual 150.0 mL beaker. Then, 50.0 mL of each mixture was taken in a 200.0 mL beaker. Afterward, it was kept at 90℃ on an electrical heater with magnetic string followed by the dropwise addition of 0.1 M NH_4OH to rise the pH of mixture up-to 10.5. At high

alkalinity, the metal ions were co-precipitated quantitatively in the form of $Sn(OH)_2.V(OH)_4{\cdot}nH_2O$ Finally, the precipitated mass was filtered to separate from aqueous medium and cleaned by the washing with deionized water and acetone successively. Subsequently, the moisture of the prepared sample was removed by keeping in an oven at 120℃ for overnight. The proposed reactions are supposed as

$$NH_4OH_{(l)}\ NH_4{}^{+}{}_{(aq)} + OH^{-}{}_{(aq)} \quad \text{(i)}$$

$$SnCl_{2(s)} \rightarrow Sn^{2+}{}_{(aq)} + 2Cl^{-}{}_{(aq)} \quad \text{(ii)}$$

$$VOSO_{4(s)} \rightarrow V^{4+}{}_{(aq)} + SO_4{}^{2-}{}_{(aq)} \quad \text{(iii)}$$

$$Sn^{2+}{}_{(aq)} + V^{4+}{}_{(aq)} + OH^{-}{}_{(aq)} + nH_2OSn(OH)_2\ .V(OH)_4{\cdot}nH_2O\downarrow \quad \text{(iv)}$$

At the end, the dry $Sn(OH)_2.V(OH)_4$ was subjected to the calcination at 500℃ around 5 h in the presence of oxygen flow by keeping inside an muffle furnace. The metal hydroxides were transformed to its oxides form ($SnO_2.V_2O_5$) with higher oxidation number due the oxidation in presence of oxygen. The corresponding reaction involves in muffle furnace as

$$Sn(OH)_2.V(OH)_4 + O_2 \rightarrow SnO_2.V_2O_5 + nH_2O\ _{(v)} \quad \text{(v)}$$

2.3. Fabrication of GCE with binary SnO_2/V_2O_5 NMs

The deposition of SnO_2/V_2O_5 NMs on GCE is the most sensitive task of this study. For this, SnO_2/V_2O_5 NMs was mixed in ethanol to result slurry and then, the gotten slurry was layered as thin film on the cross-section of GCE very carefully. It was dried by keeping at laboratory ambient condition. To establish the optimum binding strength of thin film of SnO_2/V_2O_5 NMs on GCE, the drop of nafion (5% in ethanol) was applied on it and followed by the drying again keeping inside an oven at 35.0 ℃ for an hour. To amass the proposed sensor, the Keithley electrometer was used for the constant source of volts supply and modified GCE with SnO_2/V_2O_5 NMs and Pt-wire were connected with it in series manner to the performing as working and counter electrode separately. Thiourea was thinned using demineralized water to result a range of solution as 0.1 mM ~ 0.1 nM and used as target analyte. The analytical performances such as sensitivity, linear dynamic range and detection limit were estimated from the calibration curve plotted as current vs. log (concentration of TU). The mono- & disodium phosphate were used to prepare the require buffer phase. During electrochemical investigation, the buffer solution was taken in electrochemical analyzing beaker as 10.0 mL as constant throughout the study.

Real samples (Human, Mouse, and Rabbit serum) were collected from the local medical center. All experiments were performed in compliance with relevant laws or institutional guidelines (CEAMR, King Abdulaziz University). After dilution of collected serum samples in PBS buffer, they were analyzed with the fabricated SnO_2/V_2O_5 NMs sensor by electrochemical method at room conditions. All experiments were performed in compliance with the relevant laws and institutional guidelines (Center of Excellence for Advanced Material Research at King Abdulaziz University, Jeddah, Saudi Arabia). Here we stated that All animal procedures were performed in accordance with the Guidelines for Care and Use of Laboratory Animals of "Center of Excellence for Advanced Materials Research (CEAMR)" and approved by the Animal Ethics Committee of "King Abdul Aziz University".

3. Results and discussions

3.1. XPS analysis

To investigation of binding energy and corresponding oxidation state of atom existing in synthesized NPs, X-ray Photoelectron Spectrometer (XPS) was implemented on SnO_2/V_2O_5 NMs and the resultant spectrum was illustrated in Fig. 1. Based on Fig. 1, the synthesized NPs is consist of Sn, V and O only. The core level high resolute spin orbitals of Sn3d are presented in Fig. 1(a) with binding energies of 486.5 and 495.0 eV corresponding $Sn3d_{5/2}$ and $Sn3d_{3/2}$. The energy different between two asymmetric spin orbitals of Sn3d is 8.5 eV, which is the characteristic value for oxidation state of Sn^{4+} as reported previously (Su et al., 2014; Pan et al., 2012; Zhu et al., 2016). As it is demonstrated in Fig. 1 (b), the V2p is spited into two peaks located at 516.9 and 524.2 eV respectively to $V2p_{3/2}$ and $V2p_{1/2}$ and consistent with the typical values of V^{5+} oxidation state (Wei et al., 2015; Biesinger et al., 2010; Silversmit et al., 2004). Moreover, O1s shows an intense peak at 530.4 eV, which presents O^{2-} state in SnO_2/V_2O_5 NMs and can be ascribed as lattice oxygen (Mendialdua et al., 1995; Rahman et al., 2017c; Rahman et al., 2018c).

3.2. Structural morphology of SnO_2/V_2O_5 NMs

The structural morphology of SnO_2/V_2O_5 NMs was investigated by Field-emission Scanning Electron Microscopy (FESEM) equipped with EDS and the analysis records were presented in Fig. 2. As it is perceived from Fig. 2(a-b), the prepared SnO_2/V_2O_5 NMs are consist of various structural morphology of elements with diversified shape and size. From Fig. 2(a-b), it can be concluded that the synthesized SnO_2/V_2O_5 is aggregated nanoparticles in shape. The similar observation is represented in EDS image as in Fig. 2(c). According to EDS elemental analysis report, the prepared NMs contain 41.49% O, 32.94% V and 25.57% Sn only. Any other peaks are not identified associated with impurity. Therefore, the synthesized NMs are consisted of Sn, O and V only.

3.3. Structural analysis of synthesized NMs

The powder X-ray diffraction of the as-prepared mixture metal oxides (SnO_2/V_2O_5) was obtained on Cu-Kα (λ = 1.5406 Å) in range of 2θ (0 ~ 80) shown in Fig. 3 and observed the mixt phases of SnO_2 and V_2O_5 only. The X-ray pattern of SnO_2/V_2O_5 NMs is consist of a number of SnO_2 plans and categorized as (1 0 1), (1 1 1), (1 1 0), (3 0 1), (2012), and (3 2 1), which are recognized by JCPDS card no. 0041–1445 and preceding reports (Patil et al., 2012;). Except this, the high crystalline phases of V_2O_5 are perceived in the resulted XRD pattern accredited as (0 4 0), (1 4 0), and (2 4 0) plans and conformed by JCPDS no. 0060–0767 and prior authors (Chan et al., 2014). The crystal size of the as-prepared NPs is considered by applying Scherrer Equation $D = (0.94\lambda)/(\beta Cos\theta)$ and the

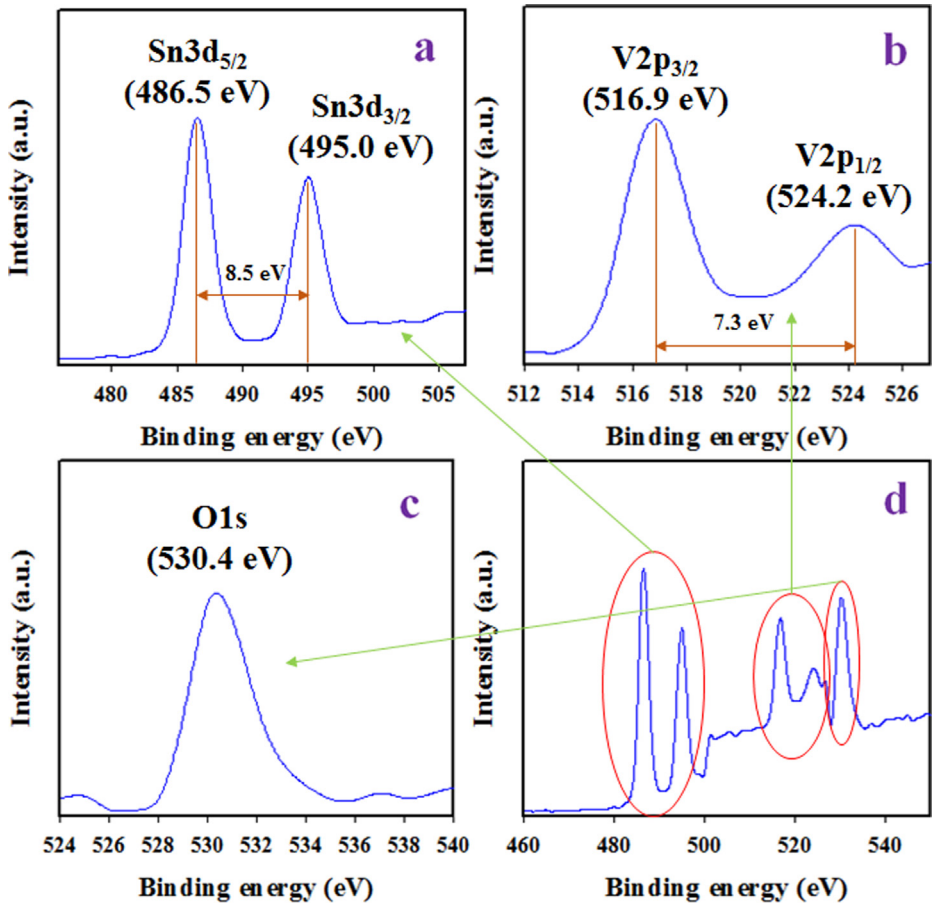

Fig. 1 XPS spectra of SnO_2/V_2O_5 NMs s which is prepared wet-chemical process. (a) High-resolution XPS of Sn3d level, (b) Asymmetric spin orbitals of V2p level, (c) O1s spectra of SnO_2/V_2O_5 NMs and (d) Survey XPS spectrum of SnO_2/V_2O_5 NMs in narrow window.

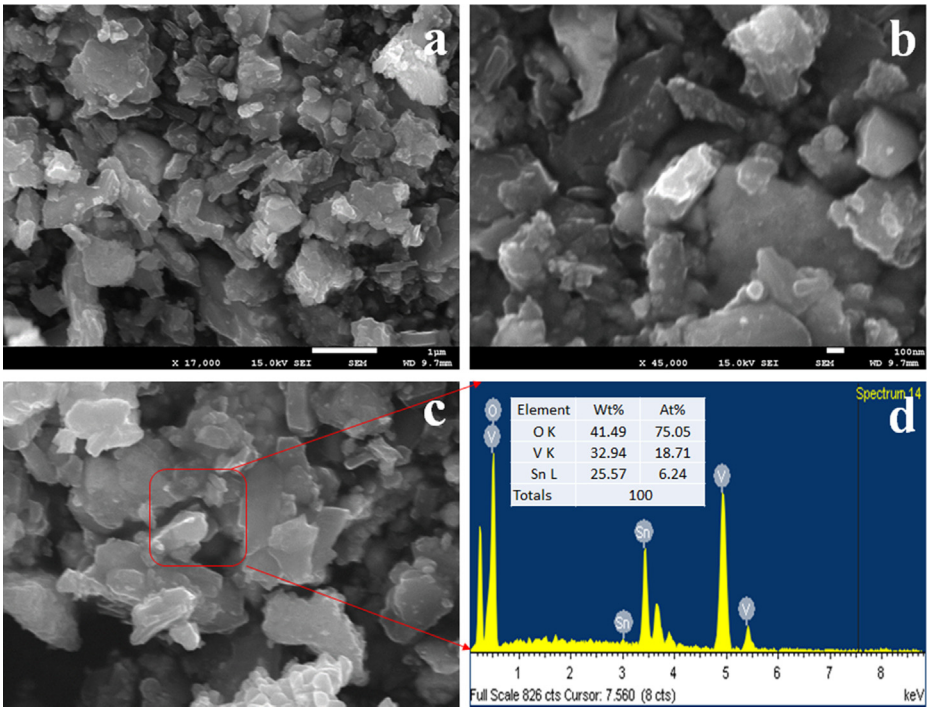

Fig. 2 Morphological and elemental analyses of SnO_2/V_2O_5 NMs. (a-b) low and high magnified FESEM images and (c-d) EDS image and elemental compositions of selected area of FESEM image.

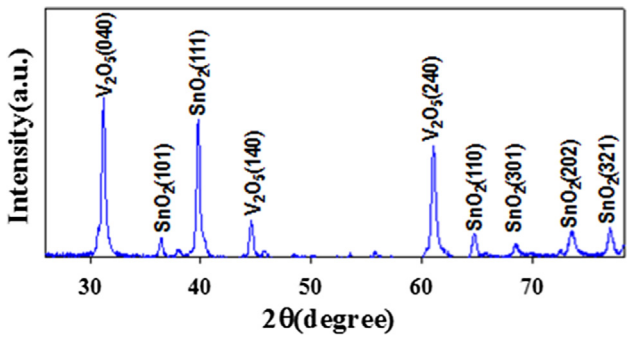

Fig. 3 Crystallinity analysis of the as-prepared NMs of SnO_2/V_2O_5 by powder XRD at room conditions.

probable crystal size using the peak of V_2O_5 (0 4 0) is equal to 21.68 nm. Herein λ (wavelength of X-ray radiation) and β (the width at half of peak)

3.4. Analytical performance of SnO_2/V_2O_5 NMs/binder/GCE sensor

The anticipated sensor was made-up as SnO_2/V_2O_5 NMs/binder/GCE sensor assembly for the detection of target biochemical. The binding strength of NMs onto GCE was coated by the addition a drop of nafion (as 5% suspension in ethanol). Since, the nafion is co-polymer having conductivity, it enhances the electron transfer rate as well as conductivity of the sensor probe during sensor application. The similar methods are already reported elsewhere, where detecting of various toxic chemicals and biochemical (Rahman et al., 2019a; Alam et al., 2019a; Abu-Zied et al., 2019; Rahman et al., 2019b) by electrochemical methods. At the starting, the sensor probe with SnO_2/V_2O_5 NMs/binder/GCE was tested in 0.1 μM of various bio-chemicals and the outcomes are presented in Fig. 4(a). These performances were investigated at pH 7.0 in the potential ranges as 0~+1.5 V. From the pictographic demonstration in Fig. 4(a), thiourea (TU) is exhibited the highest electrochemical response with SnO_2/V_2O_5 NMs/GCE. Based on the highest electrochemical response, TU is considered as the selective biochemical for the sensor assembly among the other biochemical. To optimize the pH of buffer to achieve the good electrochemical response of the sensor, it was performed in the different buffer phases of pH ranges as 5.7 ~ 8.0 by using 0.1 μM TU, which is presented in Fig. 4 (b). Obviously, TU is showed the highest electrochemical response at pH 7.0. Fig. 4(c) demonstrates the electrochemical responses of TU in a wider range of concentration from 0.1 nM to 0.1 mM (lower to higher) at pH 7.0 and in 0~+1.5 V. From the observation of Fig. 4(c), electrochemical responses are varied from low to high concentration of TU.

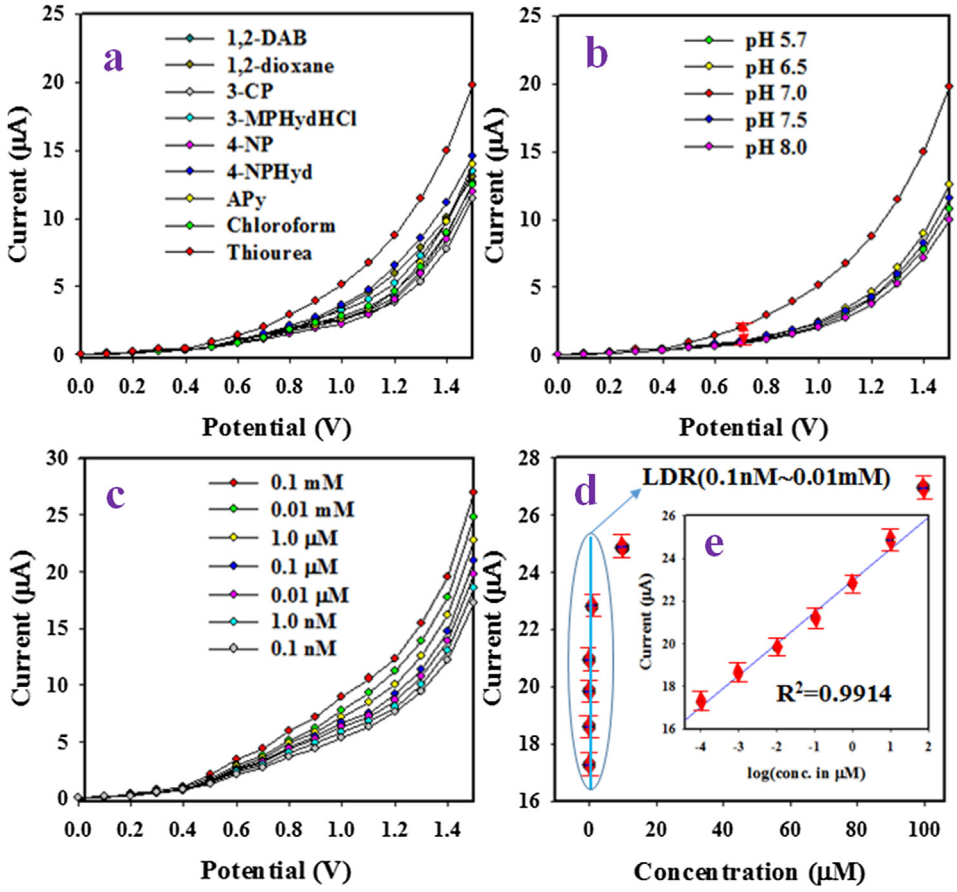

Fig. 4 Electrochemical analysis for sensor analytical performances by electrochemical method. (a) Selectivity study, (b) pH variation, (c) Sensor responses based concentration variation from lower to higher and (d) Calibration of TU sensor based on SnO_2/V_2O_5 NMs/binder/GCE [in-set current vs. log (conc.)].

The different tendencies in electrochemical responses have already described elsewhere in the detection of various toxins by applying the similar electrochemical approach (Subhan et al., 2018b; Alam et al., 2018b; Rahman et al., 2016b; Rahman et al., 2016c). Thus, it indicates that the electrochemical responses changes with the corresponding concentration of TU in a linear manner. The calibration of TU sensor is documented by plotting current verses conc. of TU as presented in Fig. 4(d). For this representation, the current data are collected from Fig. 4(c) at + 1.5 V. From the Fig. 4(d), the current are continuously increased in a linear approach correspondingly from low to high concentration of target analyte (0.1 nM ~ 0.01 mM). This range is referred as dynamic range (LDR) for the detection of TU, which is an obvious a wider range of concentration.

For the exemplification of linearity of LDR, the current data between LDR is coordinated as $y = 0.5401x + 19.689$ and regression co-efficient ($R^2 = 0.9914$). The TU sensor sensitivity is calculated by applying LDR slope by considering the surface area of GCE (0.0316 cm^2). The sensitivity is obtained from the calculation as 17.092 $\mu A \mu M^{-1} cm^{-2}$, which is evidently a higher sensitivity compared to general sensors. Applying signal–noise ratio 3, the low limit (95.40 ± 4.77 pM) of detection is also calculated. The result is significantly found very low, which is very useful for trace detection of target bio-chemicals.

To exemplify the comparison between the coated and bare GCE, the electrochemical analysis were significantly effected in buffer phase in 0~+1.5 V and 0.1 μM TU. The obtained results are presented in Fig. 5(a). It is evidently confirmed that the coated GCE by SnO_2/V_2O_5 NMs shows good electrochemical response compared to previously reported results (Khan et al., 2015; Rahman et al., 2017d; Subhan et al., 2018c). The response time of a sensor is an important parameter for sensor development. Thus, the response time of TU sensor with SnO_2/V_2O_5 NMs/binder/GCE was implemented using 0.1 μM TU in buffer phase of pH 7.0 and the corresponding obtained data are shown in Fig. 5(b). As evidenced in Fig. 5(b), the counted response time is roundly as 20.0 sec. Therefore, it is conformed that the probable TU sensor is used to the completion of electrochemical analysis within 20.0 sec. The reproducibility is a reliability indicating parameter, which defined as the capability to generate the similar electrochemical responses in the indentical conditions. Thus, this reliability parameters were examined by using 0.1 μM of TU and 0~+1.5 V in identical buffer phase. The achieved data are optimized and given in Fig. 5(c). From the outcome in Fig. 5(c), the seven electrochemical responses are almost same and not altered by the washing of working electrode after each trial. From the evidence of this performance, the TU sensor has capability to the detection of TU in the real bio-samples significantly. To having the exactness of the reproducibility performances of TU sensor, the RSD (relative standard deviation) of current data at applied volts + 1.5 V is considered and gained to 1.47% (RSD). It is confirmed the high precision of

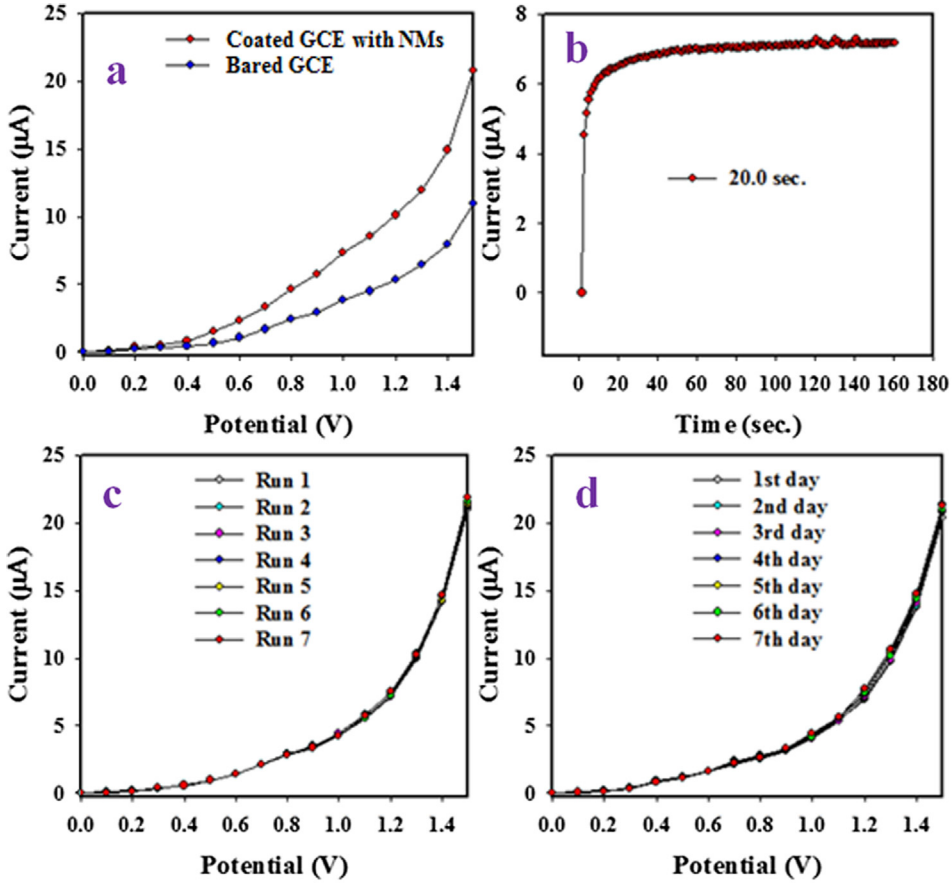

Fig. 5 Optimization of TU sensor. (a) Comparison of electrochemical response with modified GCE and bared GCE, (b) response time, (c) reproducibility and (d) Stability of TU sensor based on SnO_2/V_2O_5 NMs/binder/GCE.

Table 1 Comparative study for the detection of TU based on various materials by electrochemical methods.

Modified GCE	DL	LDR	Sensitivity	Ref.
Sn-MnO_2/CNT/GCE	0.68 μM	–	6.220 μAμ$M^{-1}cm^{-2}$	Saharan et al. 2019
CMO NPs/GCE	12.00 pM	0.1 nM ~ 1.0 mM	3.380 μA μM^{-1} cm^{-2}	Rahman et al. 2018b
SnO_2/V_2O_5 NMs/GCE	95.40 pM	0.1 nM ~ 0.01 mM	17.091 μA μM^{-1} cm^{-2}	This study

*DL (detection limit), LDR (linear dynamic range), pM(picomole), mM(millimole).

reproducibility of TU sensor. The long-term performing capability of TU sensor is essential to work in identical buffer phase. This test for TU sensor was verified by the performing of the similar tests as in the reproducibility in similar conditions around seven days. The experimented outcomes are illustrated in Fig. 5(d). The similar observation to reproducibility is apparent in this approach. Since, the deviation of electrochemical data are not perceived, it can be decided that TU sensor based on SnO_2/V_2O_5 NMs/binder/GCE is efficient enough to work with high accuracy through long period of time.

For the validation of this study, the judgement between comparable studies are very important. Therefore, the performance is presented in Table 1(Saharan et al., 2019; Rahman et al., 2018b) in term of sensitivity, LDR and DL. From the observation of Table 1, the selective TU sensor based on SnO_2/V_2O_5 NMs/binder/GCE has displayed better results compared to previously published reports.

In this approach, finally transition metal oxide co-doped nanostructure materials have employed a great deal of consideration due to their chemical, structural, physical, and optical properties in terms of large-active surface area, high-stability, high porosity, and permeability (Alam et al., 2019b; Rahman et al., 2018d; Awual et al., 2019b), which directly dependent on the structural as well as morphology prepared by reactant precursors. Here, the SnO_2/V_2O_5 nanomaterials were synthesized by a facile wet-chemical method using NH_4OH as reducing agents at ambient conditions. This technique has several advantages including facile preparation, accurate control of the reactant temperature, easy to handle, and one-step reaction. Optical, morphological, electrical, and chemical properties of SnO_2/V_2O_5 nanomaterials are of huge significance from the scientific aspect, which compared to other undoped materials (Hasnat et al., 2015; Rahman et al., 2018e; Khan et al., 2016; Rahman et al., 2018f; Sheikh et al., 2017). Non-stoichiometry, mostly oxygen vacancies, makes it conducting nature in the co-doped nanostructure materials. The formation energy of oxygen vacancies and metal interstitials in semiconductor is very low and thus these defects form eagerly, resulting in the experimentally elevated conductivity of SnO_2/V_2O_5 nanomaterials compared to other un-doped. SnO_2/V_2O_5 nanomaterials have also attracted considerable interest due to their potential applications in fabricating opto-electronics, electro-analytical, selective detection of assays, sensor devices, hybrid-composites, electron-field emission sources for emission exhibits, biochemical detections, and surface-enhanced Raman properties etc (Hussain et al., 2018; Khan et al., 2001). Therefore, SnO_2/V_2O_5 nanomaterial offers improved performances due to the large-active surface area (Rahman et al., 2017d; Rahman et al., 2017e; Rahman et al., 2017f), which increased of conductivity and current responses of SnO_2/V_2O_5 NMs/Nafion/GCE assembly during electrochemical investigation.

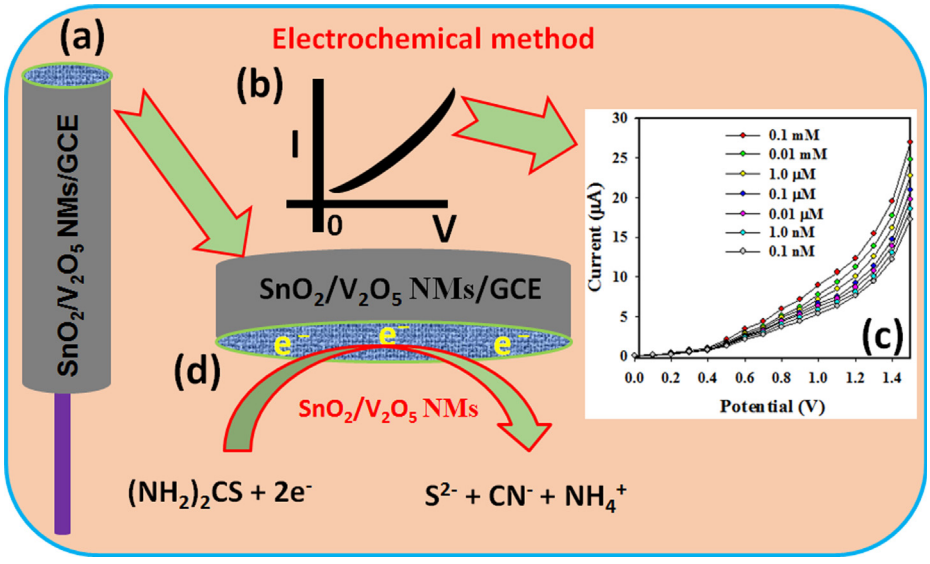

Fig. 6 Schematic representation of (a) SnO_2/V_2O_5 NMs coated rod-shaped round-GCE electrode with conducting nafion (5% ethanol) coating binders, (b) expected I-V response by the SnO_2/V_2O_5 NMs/Nafion/GCE, (c) observed I-V response by the SnO_2/V_2O_5 NMs/Nafion/GCE, and (d) proposed detection mechanism of TU, while TU is changed by removing conducting electrons from the SnO_2/V_2O_5 NMs/Nafion/GCE electrodes.

Table 2 The testing of bio-samples using SnO_2/V_2O_5 NMs/GCE sensor applying recovery system by electrochemical approach.

Sample	Added TU conc. (μM)	Measured TU conc.[a] by SnO_2/V_2O_5 NMs/binder/GCE (μM)			Average recovery[b] (%)	RSD[c] (%) (n = 3)
		R1	R2	R3		
Human Serum	0.0100	0.00985	0.00974	0.00989	98.27	0.79
Mouse Serum	0.0100	0.00974	0.00966	0.00963	96.77	0.59
Rabbit Serum	0.0100	0.00993	0.00994	0.00998	99.50	0.27

[a] Mean of three repeated determination (signal to noise ratio 3) SnO_2/V_2O_5 NMs/GCE.
[b] Concentration of TU determined/Concentration taken (Unit: μM).
[c] Relative standard deviation value indicates precision among three repeated measurements (R1,R2,R3).

Here, the selective thiourea in aqueous solution was detected and measured by using the SnO_2/V_2O_5 NMs fabricated GCE as an enzyme-less chemical sensor. Non-toxic nature, chemical stability, and electro-chemical activity make the SnO_2/V_2O_5 NMs as one of the best sensing material matrixes for the TU by electrochemical approach. Thiourea gives a remarkable response upon contact with the SnO_2/V_2O_5 NMs in the electrochemical measurement at room conditions. Fig. 6a shows the SnO_2/V_2O_5 NMs/Nafion/GCE electrode surface prepared in 5% ethanolic nafion solution. Fig. 6b represents the theoretical electrochemical I-V response. Practical I-V response with the TU in various concentration onto the SnO_2/V_2O_5 NMs/Nafion/GCE working electrode is given in Fig. 6c at a delay time of 1.0 s in the electrometer; where the higher current response to the increasing current is clearly demonstrated. Possible electrochemical changes in Scheme (Fig. 6d) onto the SnO_2/V_2O_5 NMs/Nafion/GCE is generalized in Fig. 6d; where, TU gets changed by the gaining of two electrons from the conduction band of the sensor surface during the electrochemical measurements, hence TU becomes S^{2-} ions, which ultimately increases the resultant current intensity with the increasing concentration at room conditions as in equation (i).

$$(NH_2)_2CS + 2e^- \rightarrow S^{2-} + CN^- + NH_4^+ \quad \text{(i)}$$

The interior resistance of the fabricated SnO_2/V_2O_5 NMs/Nafion/GCE sensor decreases with the decreasing electronic communication, which is an important characteristic feature of the co-doped nanomaterials at room conditions and vice versa (Wang et al., 2015; Rahman, 2020a; Rice et al., 1992). During the reaction of TU, the number of electrons in the conduction band increases and hence decreases the resistance of the SnO_2/V_2O_5 NMs. Reactions of the TU on the SnO_2/V_2O_5 NMs surface is the main phenomenon involved in this proposed TU sensor. Due to the aggregated nanostructures, SnO_2/V_2O_5 NMs have a large surface area that may be responsible for such a sensitive reduction at room temperature. The rate of the TU reaction in SnO_2/V_2O_5 NMs was higher than other nanomaterials, even under identical conditions (Rahman, 2019c; Rahman, 2018g; Rahman, 2017g). Current responses in electrochemical technique during TU detection largely depends on the dimensions, morphology, and nanoporosity of the SnO_2/V_2O_5 NMs. When SnO_2/V_2O_5 NMs surface is exposed to the oxidizing TU, surface-mediated reduction reactions take place as in equation (ii) as well as (iii) (Mozaffari et al., 2015; Rahman et al., 2019d).

$$(NH_2)_2CS + 2e^- (SnO_2/V_2O_5\ NMs) \rightarrow S^{2-} + CN^- + NH_4^+ \quad \text{(ii)}$$

$$2(NH_2)_2CS + O_2 + 4e^- (SnO_2/V_2O_5\ NMs) \rightarrow 2(NH_2)_2CO + 2S^{2-} \quad \text{(iii)}$$

Removal of the conducting electrons from the SnO_2/V_2O_5 NMs/Nafion/GCE, it increases the surface conductance of the fabricated electrode. This removal of electrons from the conduction band increases the conductance of the SnO_2/V_2O_5 NMs coating quickly. Aggregated SnO_2/V_2O_5 NMs will increase the reaction ability of the SnO_2/V_2O_5 NMs. The SnO_2/V_2O_5 NMs/Nafion/GCE sensor requires approximately 10.0 s to achieve a constant current in the electrochemical measurements. This excellent sensitivity and high electrochemical performance of the SnO_2/V_2O_5 NMs is due to the aggregated NMs that enhances the reduction of TU.

3.5. Validation of real bio-samples

The purposes of this study is to develop of a stable and reproducible enzyme-free sensor for the efficient detection of TU in various bio-samples by electrochemical method with co-doped materials, which are collected from different living objects. Thus, the TU sensor with SnO_2/V_2O_5 NMs/binder/GCE was utilized to analysis the real biochemical samples by applying recovery method. The bio-samples were collected as human, mouse and rabbit serum. As shown in Table 2, the obtained outcomes of the recovery results are quite acceptable and satisfactory.

4. Conclusion

In this approach, the SnO_2/V_2O_5 nanomaterials by applying conventional co-precipitation technique in alkaline phase was synthesized at low temperature in alkaline basic medium. The details characterization for morphological, crystalline, elemental were investigated by the using of FESEM, EDS, XRD, and XPS. The characterized SnO_2/V_2O_5 NMs were deposited by using nafion onto GCE to result the TU sensor probe fabrication. By the details experimental analyses, the TU sensor based on SnO_2/V_2O_5 NMs/nafion/GCE was exhibited a broad LDR, good sensitivity, significate low detection limit, good reproducibility, short response time and long-term stability. It was also validated wtih real bio-samples by electrochemical method at room condition by recovery method. This approach

is introduced an efficient method for introducing of new and selective enzyme-less chemical sensor probe for the detection of biochemical by electrochemical method for safety of biomedical and healthcare fields in broad scales.

Acknowledgements

Center of Excellence for Advanced Materials Research (CEAMR) at King Abdulaziz University, Saudi Arabia is highly acknowledged for the chemical sensor application facilities.

References

Abu-Zied, B.M., Alam, M.M., Asiri, A.M., Schwieger, W., Rahman, M.M., 2019. Fabrication of 1,2-dichlorobenzene sensor based on mesoporous MCM-41material. Colloid. Surface. A 562, 161–169.

Alam, M.M., Asiri, A.M., Uddin, M.T., Islam, M.A., Rahman, M.M., 2018a. Wet-chemically prepared low-dimensional $ZnO/Al_2O_3/Cr_2O_3$ nanoparticles for xanthine sensor development using an electrochemical method. RSC Adv. 8, 12562–12572.

Alam, M.M., Asiri, A.M., Uddin, M.T., Islam, M.A., Rahman, M.M., 2018b. In-situ glycine sensor development based $ZnO/Al_2O_3/Cr_2O_3$ nanoparticles. ChemistrySelect 3, 11460–11468.

Alam, M.M., Asiri, A.M., Uddin, M.T., Islam, M.A., Awual, M.R., Rahman, M.M., 2019a. Detection of uric acid based on doped $ZnO/Ag_2O/Co_3O_4$ nanoparticle loaded glassy carbon electrode. New J. Chem. 43, 8651–8659.

Alam, M.M., Asiri, A.M., Uddin, M.T., Inamuddin, Islam, M.A., Awual, M.R., Rahman, M.M., 2019. One-step wet-chemical synthesis of ternary ZnO/CuO/Co3O4 nanoparticles for sensitive and selective melamine sensor development. New J. Chem. 43, 4849-4858.

Awual, M.R., Asiri, A.M., Rahman, M.M., Alharthi, N.H., 2019a. Assessment of enhanced nitrite removal and monitoring using ligand modified stable conjugate materials. Chem. Eng. J. 363, 64–72.

Awual, M.R., Hasan, M., Asiri, A.M., Rahman, M.M., 2019b. Cleaning the arsenic(V) contaminated water for safe-guarding the public health using novel composite material. Compos. B Eng. 171, 294–301.

Baik, J.M., Kim, M.H., Larson, C., Yavuz, C.T., Stucky, G.D., Wodtke, A.M., Moskovits, M., 2009. Pd-sensitized single vanadium oxide nanowires: highly responsive hydrogen sensing based on the metal-insulator transition. Nano Lett. 9, 3980–3984.

Bhide, S.V., Deshmuh, B.T., Talvelkar, B.A., Nagvekar, A.S., 2001. Effect of induced hypothyroidism on the blood biochemical constituents in goats. Indian Vet. J. 78, 205–208.

Biesinger, M.C., Lau, L.W.M., Gerson, A.R., Smart, R., St, C., 2010. Resolving surface chemical states in XPS analysis of first row transition metals, oxides and hydroxides: Sc, Ti, V, Cu and Zn. Appl. Surf. Sci. 257, 887–898.

Bose, A.C., Kalpana, D., Thangadurai, P., Ramasamy, S., 2002. Synthesis and characterization of nanocrystalline SnO_2 and fabrication of lithium cell using nano- SnO_2. J. Power Sources 107, 138–141.

Byon, J.W., Kim, M.B., Kim, M.H., Kim, S.Y., Lee, S.H., Lee, B.C., Baik, J.M., 2012. Electrothermally induced highly responsive and highly selective vanadium oxide hydrogen sensor based on metal-insulator transition. J. Phys. Chem. C 116, 226–230.

Chan, Y.L., Pung, S.Y., Sreekantan, S., 2014. Synthesis of V_2O_5 nanoflakes on PET Fiber as visible-light-driven photocatalysts for degradation of RhB dye. J. Catal. 370696, 7.

Cooper, D.S., 1984. Antithyroid drugs. N. Engl. J. Med. 311, 1353–1362.

De Oliveira, A.N., de Santana, H., Zaia, C.T.B.V., D.A.M., 2004. A study of reaction between quinones and thiourea: determination of thiourea in orange juice. J. Food Compos. Anal. 17, 165–177.

Ezekiel, R., Vijay, P., Brajesh, S., Archana, P., Shekhawat, G.S., Paul, V., Singh, B., Peshin, A., 2000. Effect of low temperature, desprouting and gibberellic acid treatment on little tuber formation on potatoes during storage. J. Indian Potato Association. 27, 13–23.

Gholap, S.V., Dod, V.N., Bhuyar, S.A., Bharad, S.G., 2000. Effect of plant growth regulators on seed germination and seedling growth in aonla (Phyllanthus emblica L.) under climatic condition of Akola. Crop. Research Hisar. 20, 546–548.

Gilly, R., Mara, D., Oded, S., Zohar, K., 2001. Resveratrol and a novel tyrosinase in carignan grape juice. J. Agric. Food Chem. 49, 1470–1485.

Guo, D.J., 2010. Electrooxidation of ethanol on novel multi-walled carbon nanotube supported platinum–antimony tin oxide nanoparticle catalysts. J. Power Sources 196, 679–682.

Hasnat, M.A., Safwan, J.A., Islam, M.S., Rahman, Z., Karim, M.R., Pirzada, T.J., Samed, A.J., Rahman, M.M., 2015. Electrochemical decolorization of Methylene blue on Pt electrode in KCl solution for environmental remediation. J. Indust. Eng. Chem. 21, 787–791.

Heidari, R., Niknahad, H., Jamshidzadeh, A., Eghbal, M.A., Abdoli, N., 2015. An overview on the proposed mechanisms of antithyroid drugs-induced liver Injury. Adv. Pharm. Bull. 5, 1–11.

Hussain, M.M., Rahman, M.M., Asiri, A.M., 2016. Sensitive L-Leucine sensor based on a glassy carbon electrode modified with SrO nanorods. Microchim. Acta 183, 3265–3273.

Hussain, M.M., Asiri, A.M., Arshad, M.N., Rahman, M.M., 2018. Development of selective Co^{2+} ionic sensor based on various derivatives of benzenesulfonohydrazide (BSH) compounds: an electrochemical approach. Chem. Eng. J. 339, 133–143.

Khan, A., Khan, A.A.P., Rahman, M.M., Asiri, A.M., 2016a. High performance polyailine/vanadyl phosphate (PANI-$VOPO_4$) nanocomposite sheets prepared by exfoliation/intercalation method for sensing applications. European Polymer J. 75, 388–398.

Khan, A.A.P., Khan, A., Rahman, M.M., Asiri, A.M., 2016b. Conventional surfactant-doped poly(o-Anisidine)/GO nanocomposites for benzaldehyde chemical sensor development. J. Sol-Gel Sci. Technol. 77, 361–370.

Khan, A., Khan, A.A.P., Asiri, A.M., Rahman, M.M., Alhogbi, B.G., 2015. Preparation and properties of novel sol-gel-derived quaternized poly(n-methyl pyrrole)/Sn(II)SiO_3/CNT composites. J. Solid State Electrochem. 19, 1479–1489.

Karam, N.S., Al-Salem, M.M., 2001. Breaking dormancy in Arbutus andrachne L. seeds by stratification and gibberellic acid. Seed Sci. Technol. 29, 51–56.

Kargosha, K., Khanmohammadi, M., Ghadiri, M., 2001. Fourier transform infrared spectrometric determination of thiourea in the presence of sulphur dioxide in aqueous solution. Anal. Chim. Acta 437, 139–143.

Kennedy, M.K., Kruis, F.E., Fissan, H., Mehta, B.R., Stappert, S., Dumpitch, G., 2003. Tailored nanoparticle films from monosized tin oxide nanocrystals: particle synthesis, film formation, and size-dependent gas-sensing properties. J. Appl. Phys. 93, 551–560.

Khan, M.A., Ungar, I.A., 2001. Effect of germination promoting compounds on the release of primary and salt enforced seed dormancy in the halophyte Sporobolus arabicus Boiss. Seed Sci. Technol. 29, 299–306.

Kies, H.L., 1978. The conductometric titration of thiourea by mercury (II) chloride. Anal. Chim. Acta 96, 183–184.

Kosacki, I., Massot, M., Balkanski, M., Tuller, H.L., 1992. Electrical conductivity and Raman scattering of amorphous V_2O_5. Mater. Sci. Eng., B 12, 345–349.

Van, K.L., Groult, H., Mantoux, A., Perrigaud, L., Lantelme, F., Lindstrom, R., Badour- Hadjean, R., Zanna, S., Lincot, D., 2006. Amorphous vanadium oxide films synthesized by ALCVD for lithium rechargeable batteries. J. Power Sources 160, 592–601.

Lin, Y.S., Zheng, J.X., Tsui, Y.K., Yen, Y.P., 2011. Colorimetric detection of cyanide with phenyl thiourea derivatives. Spectrochim. Acta, Part A 79, 1552–1558.

Mendialdua, J., Casanova, R., Barbaux, Y., 1995. XPS studies of V_2O_5, V_6O_{13}, VO_2 and V_2O_3. Spectrosc. Relat. Phenom. 71, 249–261.

Moragues, M.E., Santos-Figueroa, Ábalos, L.E., T., Sancenón, F., Martínez-Máñez, R., 2012. Synthesis of a new tripodal chemosensor based on 2,4,6-triethyl-1,3,5-trimethylbencene scaffolding bearing thiourea and fluorescein for the chromo-fluorogenic detection of anions. Tetrahedron Lett. 53, 5110-5113.

Mozaffari, S.A., Amoli, H.S., Simorgh, S., Rahmanian, R., 2015. Impedimetric thiourea sensing in copper electrorefining bath based on DC magnetron sputtered nanosilver as highly uniform transducer. Electrochim. Acta 184, 475–482.

Pan, S.S., Wang, S., Zhang, Y.X., Luo, Y.Y., Kong, F.Y., Xu, S.C., Xu, J.M., Li, G.H., 2012. P-type conduction in nitrogen-doped SnO_2 films grown by thermal processing of tin nitride films. Appl. Phys. A 109, 267–271.

Patil, G.E., Kajale, D.D., Gaikwad, V.B., Jain, G.H., 2012. Preparation and characterization of SnO_2 nanoparticles by hydrothermal route. Int. Nano Lett. 2, 17.

Portion, E., Salle, A.L.G.A., Verbaere, A., Piffard, Y., Guyomard, D., 1999. Electrochemically synthesized vanadium oxides as lithium insertion hosts. Electrochim. Acta 45, 197–214.

Pyun, S.L., Bae, J.S., 1996. The AC impedance study of electrochemical lithium intercalation into porous vanadium oxide electrode. Electrochim. Acta 41, 919–925.

Ramana, C.V., Smith, R.J., Hussain, O.M., Massot, M., Julien, C.M., 2005. Surface analysis of pulsed laser-deposited V_2O_5 thin films and their lithium intercalated products studied by Raman spectroscopy. Surf. Interface Anal. 37, 406–411.

Rahman, M.M., Khan, A., Asiri, A.M., 2015. Chemical sensor development based on poly(o-anisidine)silverized-MWCNT nanocomposites deposited glassy carbon electrodes for environmental remediation. RSC Adv. 5, 71370–71378.

Rahman, M.M., Balkhoyor, H.B., Asiri, A.M., 2016a. Ultrasensitive and selective hydrazine sensor development based on Sn/ZnO nanoparticles. RSC Adv. 6, 29342–29352.

Rahman, M.M., Hussain, M.M., Asiri, A.M., 2016b. A glutathione biosensor based on a glassy carbon electrode modified with CdO nanoparticles-decorated carbon nanotube in a nafion matrix. Microchim. Acta 183, 3255–3263.

Rahman, M.M., Ahmed, J., Asiri, A.M., Hasnat, M.A., Siddiquey, I. A., 2016c. Development of 4-methoxyphenol chemical sensor based on NiS_2-CNT nanocomposites. J. Taiwan Inst. Chem. Eng. 64, 157–165.

Rahman, M.M., Alam, M.M., Asiri, A.M., Islam, M.A., 2017a. Fabrication of selective chemical sensor with ternary $ZnO/SnO_2/Yb_2O_3$ nanoparticles. Talanta 170, 215–223.

Rahman, M.M., Ahmed, J., Asiri, A.M., 2017b. Development of Creatine sensor based on antimony-doped tin oxide (ATO) nanoparticles. Sens. Actuators, B Chem. 242, 167–175.

Rahman, M.M., Alam, M.M., Asiri, A.M., 2017c. Fabrication of an acetone sensor based on facile ternary $MnO_2/Gd_2O_3/SnO_2$ nanosheets for environmental safety. New J. Chem. 41, 9938–9946.

Rahman, M.M., Hussain, M.M., Asiri, A.M., 2017d. Fabrication of 3-methoxyphenol sensor based on Fe3O4 decorated carbon nanotube nanocomposites for environmental safety: real sample analyses. PLoS ONE 12, e0177817.

Rahman, M.M., Alam, M.M., Asiri, A.M., Awual, M.R., 2017e. Fabrication of 4-aminophenol sensor based on hydrothermally prepared ZnO/Yb_2O_3 nanosheets. New J. Chem. 41, 9159–9169.

Rahman, M.M., Hussain, M.M., Asiri, A.M., 2017f. Bilirubin sensor based on CuO-CdO composites deposited in a nafion/glassy carbon electrode matrixes. Progr. Nat. Sci.: Mater. Inter. 27, 566–573.

Rahman, M.M., Alam, M.M., Asiri, A.M., Awual, M.R., 2017g. Fabrication of 4-aminophenol sensor based on hydrothermally prepared ZnO/Yb_2O_3 nanosheets. New J. Chem. 41, 9159–9169.

Rahman, M.M., Alam, M.M., Asiri, A.M., 2018. Selective hydrazine sensor fabrication with facile low-dimensional Fe_2O_3/CeO_2 nanocubes. New J. Chem. 42, 10263–10270.

Rahman, M.M., Ahmed, J., Asiri, A.M., 2018b. Thiourea sensor development based on hydrothermally prepared CMO nanoparticles for environmental safety. Biosens. Bioelectron. 99, 586–592.

Rahman, M.M., Alam, M.M., Asiri, A.M., 2018c. Sensitive 1,2-dichlorobenzene chemi-sensor development based on solvothermally prepared FeO/CdO nanocubes for environmental safety. J. Indust. Engineering Chem. 62, 392–400.

Rahman, M.M., Alam, M.M., Asiri, A.M., 2018d. Carbon black co-adsorbed ZnO nanocomposites for selective benzaldehyde sensor development by electrochemical approach for environmental safety. J. Indust. Engineering Chem. 65, 300–308.

Rahman, M.M., Alam, M.M., Asiri, A.M., Islam, M.A., 2018e. 3,4-Diaminotoluene sensor development based on hydrothermally prepared MnCoxOy nanoparticles. Talanta 176, 17–25.

Rahman, M.M., 2018. A label-free Kanamycin sensor development based on CuO-NiO Hollow-spheres: food samples analyses. Sens. Actuators: B Chem. 264, 84–91.

Rahman, M.M., Alam, M.M., Asiri, A.M., 2019a. Detection of toxic choline based on Mn_2O_3/NiO nanomaterials by an electrochemical method. RSC Adv. 9, 35146–35157.

Rahman, M.M., Hussain, M.M., Arshad, M.N., Awual, M.R., Asiri, A.M., 2019b. Arsenic sensor development based on modified with (E)-N′-(2-Nitrobenzylidine)-benzenesulfonohydrazide: A real sample analysis. New J. Chem. 43, 9066–9075.

Rahman, M.M., Sheikh, T.A., Asiri, A.M., Awual, M.R., 2019d. Development of 3-methoxyaniline sensor probe based on thin $Ag_2O@La_2O_3$nanosheets for environmental safety. New J. Chem. 43, 4620–4632.

Rahman, M.M., 2020. Efficient formaldehyde sensor development based on Cu-codoped ZnO nanomaterial by an electrochemical approach. Sens. Actuators B Chem. 305, 127541.

Rethmeier, J., Neumann, G., Stumpf, C., Rabenstein, A., Vogt, C., 2001. Determination of low thiourea concentrations in industrial process water and natural samples using reversed- phase high-performance liquid chromatography. J. Chromatogr. A 934, 129–134.

Rice, D.A., Hibble, S.J., Almond, M.J., Mohammad, K.A.H., Pearse, S.P., 1992. J. Mater. Chem. 2, 895–896.

Saharan, P., Sharm, A.K., Kumar, V., Kaushal, I., 2019. Multifunctional CNT supported metal doped MnO_2 composite for adsorptive removal of anionic dye and thiourea sensing. Mater. Chem. Phys. 221, 239–249.

Schneider, K., Lubeck, M., Czapla, A., 2016. V_2O_5 thin films for gas sensor applications. Sens. Actuators, B 236, 970–977.

Siddiq, M., Cash, J.N., Sinha, N.K., Akhter, P., 1994. Characterization and inhibition of polyphenol oxidase from pears. J. Food Biochem. 17, 327–337.

Silversmit, G., Depla, D., Poelman, H., Marin, G.B., Gryse, R.D., 2004. Determination of the V2p XPS binding energies for different vanadium oxidation states (V^{5+} to V^{0+}). J. Electron Spectrosc. Relat. Phenom. 135, 167–175.

Sheikh, T.A., Arshad, M.N., Rahman, M.M., Asiri, A.M., Marwani, H.M., Awual, M.R., Bawazir, W.A., 2017. Trace electrochemical detection of Ni^{2+} ions with bidentate N, N'-(ethane-1,2-diyl)bis (3,4-dimethoxybenzenesulfonamide) [EDBDMBS] as a chelating agent. Inorganica Chim. Acta 464, 157–166.

Sohan, S., Bindra, A.S., Cheema, S.S., Dhillon, W.S., 1991. Induction of early ripening in grapes cv. Perlete. J. Plant Sci. Res. 7, 40–41.

Sokkar, S.M., Soror, A.H., Ahmed, Y.F., Ezzo, O.H., Hamouda, M. A., 2000. Pathological and biochemical studies on experimental hypothyroidism in growing lambs. J. Vet. Med Ser. B 47, 641–652.

Subhan, M.A., Saha, P.C., Sumon, S.A., Ahmed, J., Asiri, A.M., Rahman, M.M., Al-Mamun, M., 2018a. Enhanced photocatalytic activity and ultra-sensitive benzaldehyde sensing performance of a SnO_2·ZnO·TiO_2 nanomaterial. RSC Adv. 8, 33048–33058.

Subhan, M.A., Saha, P.C., Alam, M.M., Asiri, A.M., Al-Mamun, M., Rahman, M.M., 2018b. Development of bis-phenol A sensor based on Fe_2MoO_4·Fe_3O_4·Zn onanoparticles for sustainable environment. J. Environ. Chem. Eng. 6, 1396–1403.

Subhan, M.A., Saha, P.C., Rahman, M.M., Ahmed, J., Asiri, A.M., Al-Mamun, M., 2018c. Fabrication of a 2,4-dinitrophenol sensor based on Fe_3O_4@Ag@Ni nanomaterials and studies of their antibacterial properties. New J. Chem. 42, 872–881.

Su, S.C., Zhang, H.Y., Zhao, L.Z., He, M., Ling, C.C., 2014. Band alignment of n-SnO_2/p- GaN hetero-junction studied by x-ray photoelectron spectroscopy. J. Phys. D Appl. Phys. 47, 215102.

US Department of Health and Human Services, 1985. Fourth Annual Report on Carcinogens. Washington DC 423.

Wang, J., Fan, H., Yu, H., 2015a. Synthesis of monodisperse walnut-like SnO_2 spheres and their photocatalytic performances. J. Nanomater. 395483, 8.

Wang, D.Y., Gong, M., Chou, H.L., Pan, C.J., Chen, H.A., Wu, Y., Lin, M.C., Guan, M., Yang, J., Chen, C.W., Wang, Y.L., Hwang, B.J., Chen, C.C., Dai, H., 2015b. J. Am. Chem. Soc. 137, 1587–1592.

Wang, Y., Takahashi, K., Lee, L., Cao, G., 2006. Nanostructured vanadium oxide electrodes for enhanced lithium-ion intercalation. Adv. Funct. Mater. 16, 1133–1144.

Wei, Q., Liu, J., Feng, W., Sheng, J., Tian, X., He, L., An, Q., Mai, L., 2015. Hydrated vanadium pentoxide with superior sodium storage capacity. J. Mater. Chem. A 3, 8070–8075.

WHO, 2000. Pesticides residues in food Part II. Geneva. Switzerland: World Health Organization.

Wruck, D., Ramamurthi, S., Rubin, S., 1989. Sputtered electrochromic V_2O_5 films. Thin Solid Films 182, 79–86.

You, D.J., Kwon, K., Pak, C., Chang, H., 2009. Platinum–antimony tin oxide nanoparticle as cathode catalyst for direct methanol fuel cell. Catal. Today 146, 15–19.

Zhang, D., Yang, Z., Wu, Z., Dong, G., 2019a. Metal-organic frameworks-derived hollow zinc oxide/cobalt oxide nanoheterostructure for highly sensitive acetone sensing. Sens. Actuators, B Chem. 283, 42–51.

Zhang, D., Cao, Y., Wu, J., Zhang, X., 2020. Tungsten trioxide nanoparticles decorated tungsten disulfide nanoheterojunction for highly sensitive ethanol gas sensing application. Appl. Surf. Sci. 503, 144063.

Zhang, D., Wu, J., Li, P., Cao, Y., Yang, Z., 2019b. Hierarchical nanoheterostructure of tungsten disulfide nanoflowers doped with zinc oxide hollow spheres: benzene gas sensing properties and first-principles study. ACS Appl. Mater. Interf. 11, 31245–31256.

Zhang, D., Wu, J., Cao, Y., 2019c. Ultrasensitive H2S gas detection at room temperature based on copper oxide/molybdenum disulfide nanocomposite with synergistic effect. Sens. Actuators, B Chem. 287, 346–355.

Zhu, H., Rosenfeld, D.C., Harb, M., Anjum, D.H., Hedhili, M.N., Chikh, S.O., Basset, J.M., 2016. Ni−M−O (M = Sn, Ti, W) catalysts prepared by a dry mixing method for oxidative dehydrogenation of ethane. ACS Catal. 6, 2852–2866.